Received: 23 December 2020 | Revised: 17 March 2021 | Accepted: 2 April 2021

DOI: 10.1002/ajmg.a.62224

ORIGINAL ARTICLE

AMERICAN JOURNAL OF medical genetics PART A WILEY

Microdeletion of 9q22.3: A patient with minimal deletion size associated with a severe phenotype

Adam D. Ewing[1] | Seth W. Cheetham[1] | James J. McGill[2] | Michael Sharkey[3] | Rick Walker[4,5] | Jennifer A. West[6] | Malcolm J. West[6] | Kim M. Summers[1]

[1]Mater Research Institute-University of Queensland, Translational Research Institute, Woolloongabba, Queensland, Australia

[2]Department of Chemical Pathology, Royal Brisbane and Women's Hospital, Herston, Queensland, Australia

[3]Paddington Dermatology Specialist Clinic, Paddington, Queensland, Australia

[4]QLD Youth Cancer Service, Queensland Children's Hospital, South Brisbane, Queensland, Australia

[5]School of Clinical Medicine, The University of Queensland, Herston, Queensland, Australia

[6]Northside Clinical School, Prince Charles Hospital, The University of Queensland, Chermside, Queensland, Australia

Correspondence
Kim M. Summers, Mater Research Institute-UQ, Translational Research Institute, 37 Kent St, Woolloongabba, QLD 4102, Australia.
Email: kim.summers@mater.uq.edu.au

Funding information
National Health and Medical Research Council, Grant/Award Number: GNT1161832

Abstract

Basal cell nevus syndrome (also known as Gorlin Syndrome; MIM109400) is an autosomal dominant disorder characterized by recurrent pathological features such as basal cell carcinomas and odontogenic keratocysts as well as skeletal abnormalities. Most affected individuals have point mutations or small insertions or deletions within the *PTCH1* gene on human chromosome 9, but there are some cases with more extensive deletion of the region, usually including the neighboring *FANCC* and/or *ERCC6L2* genes. We report a 16-year-old patient with a deletion of approximately 400,000 bases which removes only *PTCH1* and some non-coding RNA genes but leaves *FANCC* and *ERCC6L2* intact. In spite of the small amount of DNA for which he is haploid, his phenotype is more extreme than many individuals with longer deletions in the region. This includes early presentation with a large number of basal cell nevi and other skin lesions, multiple jaw keratocysts, and macrosomia. We found that the deletion was in the paternal chromosome, in common with other macrosomia cases. Using public databases, we have examined possible interactions between sequences within and outside the deletion and speculate that a regulatory relationship exists with flanking genes, which is unbalanced by the deletion, resulting in abnormal activation or repression of the target genes and hence the severity of the phenotype.

KEYWORDS
9q22.3 deletion, basal cell nevus syndrome, Gorlin syndrome, *PTCH1*

1 | INTRODUCTION

Basal Cell Nevus Syndrome (BCNS, also known as Gorlin Syndrome; MIM109400) is an autosomal dominant disorder characterized by craniofacial and skeletal abnormalities and recurrent pathological features such as basal cell carcinomas (BCCs) and odontogenic keratocysts (Gorlin, 2004; Thalakoti & Geller, 2015). Ectopic calcification is also very prevalent. Affected individuals usually have pits on the palms and soles and have distinctive facial features including frontal bossing and macrocephaly. There is a wide variability in the manifestations of BCNS, and affected individuals can also develop other tumors and cancers including tumors of the central nervous system, particularly medulloblastoma (Evans & Farndon, 2002 [updated 2018]; Malbari & Lindsay, 2020). However, some affected individuals have minimal signs with very few BCCs or other lesions (Gorlin, 2004). BCNS is usually caused by a mutation in the *PTCH1* gene (encoding patched 1; MIM601309) on the long arm of chromosome 9 (9q22.32), although similar phenotypes have been reported

with mutations within *SUFU* (suppressor of fused homolog, located at 10q24.32; MIM607035) (Pastorino et al., 2009) and possibly *PTCH2* (patched 2, located at 1p34.1; MIM603673) (Altaraihi et al., 2019; Fan et al., 2008; Fujii et al., 2013; Pastorino et al., 2009). These proteins regulate signaling through the hedgehog pathway, which mediates key developmental processes in the embryo and continues to be active in some cell types after birth.

The majority of cases of BCNS involve single base changes or small insertion/deletion (indel) variants of *PTCH1* (Evans et al., 2017; Reinders et al., 2018; Soufir et al., 2006; Wicking et al., 1997) (mutations listed at http://www.lovd.nl/ptch1). Up to 13% of BCNS cases have deletions of at least one exon (Evans et al., 2017) and a small proportion of these have larger deletions of chromosome 9 encompassing *PTCH1* as well as additional material. The longest reported such deletion to date is 20.5 mb while the shortest is 0.35 mb (Boonen et al., 2005; Brickler et al., 2014; Cajaiba et al., 2006; Cayrol et al., 2019; Garavelli et al., 2013; Isidor et al., 2013; Kieny et al., 2018; Muller et al., 2012; Redon et al., 2006; Reichert et al., 2015; Shimojima et al., 2009; Yamada et al., 2020). As with other microdeletion syndromes (Schmickel, 1986; Weise et al., 2012), most patients with 9q22.3 deletion have multiple signs and symptoms in addition to the manifestations of BCNS. These include hydrocephalus, premature fusion of the metopic suture or trigonocephaly, macrosomia, and global delay. These features may be attributed to the deletion of genes in addition to *PTCH1*. In particular in almost all reported cases the deletion encompasses all or part of the neighboring Fanconi anemia complementation group C (*FANCC*) gene (Gibson et al., 1994), potentially predisposing these individuals to the clinical manifestations of the recessive condition Fanconi anemia (MIM227645). Another gene that is frequently included in the deletion is *TGFBR1* (9q22.33), associated with the dominant condition Loeys-Dietz syndrome type 1 (MIM609192) (Loeys et al., 2005) and a recessive condition involving susceptibility to multiple self-healing squamous epitheliomas (MIM132800) (Goudie et al., 2011). Most patients with 9q22.3 deletions have intellectual disabilities, in common with other microdeletions (Schmickel, 1986; Weise et al., 2012), although those with the smallest deletions may have normal intellectual function (for example, Case 10 from Muller and colleagues; Muller et al., 2012).

We report a patient with a short 9q22.3 deletion covering *PTCH1* and several neighboring non-coding RNA genes, accompanied by severe BCNS and other manifestations of 9q22.3 microdeletion, but without intellectual disability.

2 | CLINICAL REPORT

2.1 | Clinical history

The patient is a 16-year-old boy, the second child of non-consanguineous parents with no relevant family history. The pregnancy was notable for a rapidly growing fetal head. He was delivered at 36 weeks by Caesarean section due to maternal hypertension. Birth weight was 3.76 kg (97th percentile for gestational age; Dobbins et al., 2012), length was 51.5 cm (75th percentile for full term; https://www.who.int/childgrowth/standards/en/), head circumference was 37.7 cm (99th percentile for full term; https://www.who.int/childgrowth/standards/en/). The baby was placed in a humidicrib and received oxygen for 3 days. At 6 weeks old, he was diagnosed with communicating hydrocephalus of unknown origin. Surgery for hydrocephalus was undertaken at 7 months to insert a VP shunt. Figure 1(a) shows the patient at age 7 months immediately after surgery, where the large head is apparent, and Figure 1 (b) shows the increasing head circumference over the first 2 years of life. Gross and fine motor developmental milestones were delayed along with speech. He crawled at 15 months of age and walked at approximately 18 months of age. At 2.5 years of age, he was not talking and was diagnosed with childhood apraxia of speech. He received physiotherapy, occupational therapy, and speech therapy and currently at age 16 years has no difficulty with speech. At 4 years of age, he was diagnosed with scoliosis and Sprengel deformity of the shoulders (https://rarediseases.info.nih.gov/diseases/7693/sprengel-deformity). X-ray examination revealed fused ribs and abnormalities in his spine. At 11 years 1 month MRI of the spine showed early disc degeneration in L3/L4 as well as upper thoracic asymmetry (convex left, centered at T3) and fused 4th and 5th ribs. Calcification of the falx was confirmed with MRI examination.

The presence of skin lesions was noticed by the parents from about 4 years of age. BCCs were first diagnosed clinically at age 10 years 3 months. Between then and age 16 years he had a total of 138 lesions removed, of which 58 were shown to be BCCs, 29 were trichoepitheliomas with the potential to progress to BCCs and the remainder were a range of other lesions, including skin tags and benign pigmented naevi. BCCs have been removed from arms, fingers, shoulders, back, neck, clavicle, scalp, popliteal fossa, groin, and abdomen. Keratocystic odontogenic tumors (KCOT) were first detected at 9 years 6 months. All permanent teeth were visible except for one wisdom tooth. Several teeth were displaced. A total of nine KCOT have been removed, along with eight teeth.

His height and weight tracked with the 97th centile for age from age 4 months (Figure 1(c),(d)). At age 16 years, his height is 184 cm (90th centile for age) and weight is 86 kg (97th centile for age). Puberty is currently well advanced. Head circumference at 16 years is 63.5 cm (> 98th centile for adults; Figure 1(b)). He shows no sign of intellectual disability. He attends a local high school and has achieved his academic milestones with a grade point average above the average for his peers.

Father's adult height is 176 cm and mother's adult height is 168 cm. Predicted height for a male offspring is 178.5 cm (see Figure 1(c)). Father's adult head circumference is 58 cm and mother's adult head circumference is 55.5 cm. The parents and siblings show no signs of BCNS.

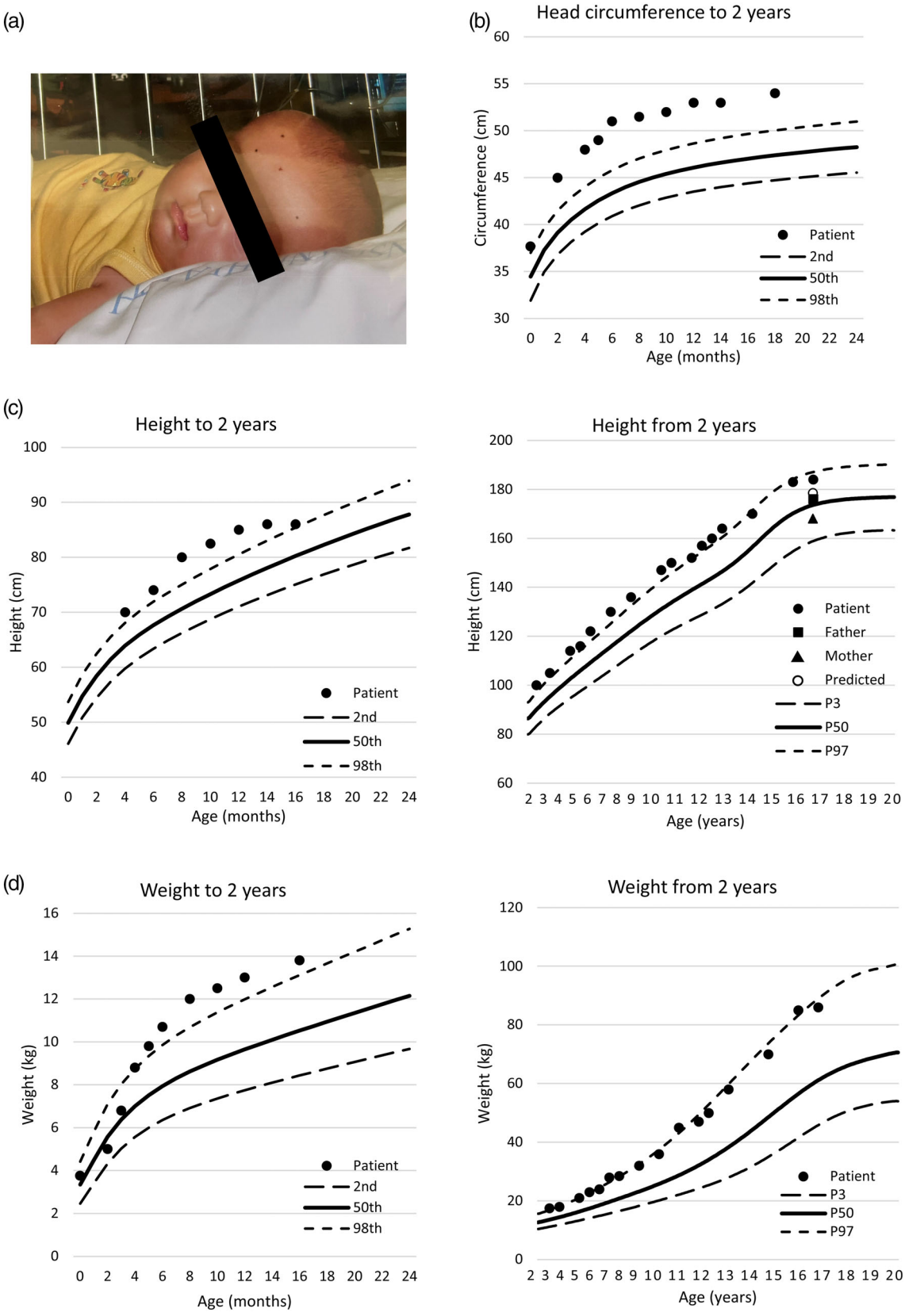

FIGURE 1 9q22.3 deletion patient. (a) Patient at 7 months of age, at the time of placement of the VP shunt. Note, dots on forehead are location marks from surgery. (b) Head circumference birth to 2 years. Circumference at 16 years is 63.5 cm. (c) Height charts; left birth to 2 years, right 2 to 16 years. Triangle—mother's adult height; square—father's adult height; open dot—predicted adult height. (d) Weight charts; left birth to 2 years, right 2 to 16 years. Data for growth charts were derived from CDC data from 2000 to 2007 (http://www.cdc.gov/growthcharts) as presented in spreadsheets available at https://www.seattlechildrens.org/about/community-benefit/obesity-program/education-for-healthcare-providers/excel-based-clinical-tools-assist-growth-charts/. Predicted adult height calculated from a formula provided in the same resource [Color figure can be viewed at wileyonlinelibrary.com]

2.2 | Treatment

To date, the treatment has consisted of regular skin surveillance, surgery to remove BCCs and KCOTs, together with avoidance of exposure to sunlight. The patient has been taking a daily supplement of nicotinamide (vitamin B3) for 2 years. Other clinical signs and symptoms are treated by conventional therapies. The possible use of hedgehog inhibitors as a way to manage the condition in the future has been reviewed, although there are undesirable side effects and hedgehog pathway inhibitors are contraindicated in children (Kieran et al., 2017; Robinson et al., 2017).

2.3 | Genetic analysis

Although the boy showed abnormalities in multiple systems, initial assessment at age 4 years suggested that he did not have any clinical syndrome warranting genetic testing. At 9 years 5 months, multiplex ligation-dependent probe amplification (MLPA) analysis of DNA was undertaken at West Midlands Regional Genetics Laboratory, UK, and it was determined that there was a heterozygous pathogenic deletion of exons 1 to 24 of the *PTCH1* gene. He was given a diagnosis of BCNS. At age 10 years 10 months, further genetic testing was undertaken at Yale-New Haven Hospital, using chromosome microarray comparative genomic hybridization (CGH) (Agilent 180 K). The results revealed a 364Kb deletion (mapped to version GRCh37 of the human genome reference sequence) at 9q22.32, including the *PTCH1* gene. The CGH microarray analysis of the parents was normal. Whole genome sequencing of the patient's DNA (performed by Genome One, Sydney, Australia) reported no other clinically significant variants relevant to the phenotype.

3 | METHODS

3.1 | Editorial policies and ethical considerations

The study was approved by Mater Misericordiae Ltd Human Research Ethics Committee (EC00332), approval number HREC/MML/45819 (V3), and conforms to the Australian Government National Statement on Ethical Conduct in Human Research (2007)—Updated 2018. All family members gave informed consent prior to participating in this research.

3.2 | Bioinformatic analysis

The patient's whole genome was initially sequenced by a commercial company (Genome One) from blood DNA and the FASTQ files were supplied. Reads were aligned to human genome reference sequence GRCh38 (GATK Resource Bundle) using bwa-mem version 0.7.12 (Li, 2013). Duplicate reads were marked using picard tools and indels were realigned using GATK 3.7 (McKenna et al., 2010). Single nucleotide variants (SNVs) and indels were detected with HaplotypeCaller from GATK 3.7. Structural variants including deletions, duplications, insertions, inversions, and translocations were detected with Delly version 0.7.7 (Rausch et al., 2012).

Genes within the deleted region were retrieved using Ensembl BioMart (http://www.ensembl.org/biomart/martview/). The significance of variants was determined using the variant effect predictor from Ensembl (http://www.ensembl.org/info/docs/tools/vep/index.html) which presents results of SIFT and PolyPhen analysis (McLaren et al., 2016), and using the ClinVar database (https://www.ncbi.nlm.nih.gov/clinvar/), an archive of reports of relationships among human variants and phenotypes (Landrum et al., 2018; Landrum & Kattman, 2018). Population allele frequencies and the common allele for variants were determined using the Genome Aggregation Database (gnomAD–Genomes) for Europeans, to most closely reflect the genetic backgrounds of the parents. The details were taken from dbSNP (https://www.ncbi.nlm.nih.gov/snp/). Bioinformatic analysis of regulatory relationships involving the deleted region used The GeneHancer Regulatory Elements section of GeneCards (https://www.genecards.org; accessed July 2020) which describes genomic regulatory elements related to the selected gene. GeneHancer is a database of genome-wide enhancer-to-gene and promoter-to-gene associations (Fishilevich et al., 2017). Regulatory elements are mined from The ENCODE Project (ENCODE Project Consortium, 2012), Ensembl regulatory build (Zerbino et al., 2015), FANTOM5 atlas of active enhancers (Andersson et al., 2014), VISTA enhancer browser (Visel et al., 2007), dbSUPER (Khan & Zhang, 2016), EPDnew (Dreos et al., 2013), UCNEbase (Dimitrieva & Bucher, 2013), and the craniofacial atlas (Wilderman et al., 2018). We also accessed the compendium of chromatin interactions provided by Jung and colleagues (Jung et al., 2019). The FANTOM5 dataset (Forrest et al., 2014), available at https://fantom.gsc.riken.jp/zenbu/ was used to determine promoter regions and gene expression levels. To examine the potential regulatory sequence *FANCC-203*, PacBio Iso-Seq cDNA-sequencing data from mixed cell lines were downloaded from https://downloads.pacbcloud.com/public/dataset/UHR_IsoSeq/. Full-length reads were aligned to the human genome (GRCh38) using Minimap2 (https://doi.org/10.1093/bioinformatics/bty191).

3.3 | Determination of parent of origin

Saliva samples were collected from the patient and his parents using OG-500 tubes (DNA Genotek, Ottawa, Canada) and DNA extracted according to manufacturer's instructions with the reagents supplied. Polymerase chain reaction (PCR) was used to amplify regions of the deletion containing potential segregating SNVs. The PCR contained 1 unit of MyTaq *Taq* polymerase (Meridian Bioscience, Sydney, Australia), 0.5 μM each primer, and 1 ng/μl template DNA in the manufacturer's MyTaq reaction buffer. PCR conditions were 1 min at 94 C

followed by 30 cycles of 0.25 min at 94 C, 0.25 min at 60 C, and 0.5 min at 72 C. This was followed by 10 min at 72 C and the samples were then held at 10 C. PCR products were sent to the Australian Genome Research Facility, University of Queensland, Brisbane, Australia for cleanup and chain termination (Sanger) sequencing. Primers and variant alleles are listed in Table 1.

4 | RESULTS

4.1 | Genes within the deletion

To further understand the extent of the deletion, the whole genome sequence data were mapped to GRCh38 and the deletion was determined to extend from 9:95,403,395 to 9:95,804,680 (401,286 bases) (Figure 2(a), Supplementary Figure S1). Analysis of public databases showed that the deleted region contained the whole of the *PTCH1* gene plus several long non-coding RNAs and two pseudogenes (Figure 2(b)). Unlike the majority of 9q22.3 microdeletions, this deletion did not include the *FANCC* gene (encoding a protein of the Fanconi anemia DNA repair complex), although two non-coding transcripts attributed to *FANCC* were within the deleted region. *FANCC-203* (ENST00000433644.2) is a short processed transcript wholly within the deletion; *FANCC-212* (ENST00000636777.1) is a longer processed transcript where the promoter region and initial exon were within the deletion. In addition, the *ERCC6L2* gene was beyond the distal breakpoint while a long non-coding RNA gene (*LINC00476*) was partially deleted. Analysis of three SNVs across the deleted region (indicated by arrows in Figure 2(a)) showed that the mother was heterozygous while the father was homozygous for the common allele. In each case, the patient had inherited the rare allele from the mother and no allele from the father, indicating that the deletion had occurred in the paternal chromosome (Figure 3).

One explanation for the variable phenotype is that the deletion exposed recessive variants in the haploid region. Given the extreme BCNS phenotype and since *PTCH1*, located at 9:95,442,980-95,517,057, is the only known protein coding gene in the deletion (Figure 2(b)), we examined the variants in the remaining maternal *PTCH1* allele. There were five variants that were different from the reference sequence, four being known SNVs where the proband carried an allele that is common in Europeans, and one was a novel variant. Four were intronic and one was in the 3′ UTR and all were considered benign or not reported as clinical variants. There were no protein coding variants in the maternal *PTCH1* (Supplementary Table S1). Other genes within the deletion are transcribed into non-coding RNAs. These include *FANCC-203* (ENST00000433644.2), which is highly expressed in cancer cell lines (FANTOM5 database; https://fantom.gsc.riken.jp/zenbu; see Supplementary Figure S2). *FANCC-203* is transcribed into a variety of isoforms, not all annotated in ENSEMBL (Supplementary Figure S3). The *FANCC-203* promoter is highly conserved and can act as a rare alternative promoter for the major *FANCC* gene, overlapping *FANCC-212* (Figure 2, Supplementary Figure S3). The patient differed from the GRCh38 reference sequence for nine variants within *FANCC-203*, two in the promoter region (rs357521, T > A, frequency of A in Europeans = 0.38; rs357522, G > A, frequency of A in Europeans = 0.68) (Supplementary Table S2). The significance of these variants is unclear.

4.2 | Variants in members of the hedgehog signaling pathway

We then considered whether there might be detrimental variants in other members of the hedgehog signaling pathway by examining the sequence of hedgehog pathway genes listed previously (Onodera et al., 2017). Protein coding variants are shown in Supplementary Table S3. Although a number of coding sequence variants were present, the majority were known variants with appreciable frequencies in the general population, and in regions/codons that are not highly conserved. The patient was heterozygous for most of these. There were four deleterious/probably or possibly damaging variants. Three of these had conflicting predictions across SIFT, PolyPhen, and ClinVar. One was rs4667591 (in *LRP2*, MIM600073) where the patient was homozygous for the common allele and it seems unlikely that this would contribute to his phenotype. For rs1567047 (in *FAT4*, MIM612411), the patient was homozygous for the rarer allele (allele frequency 0.28). He was heterozygous for

TABLE 1 Variant genotyping

SNV ID	Position	Rare allele[a]	Frequency of rare allele[a]	Patient allele	Primers (5′–3′)
rs45619434	9:95,480,278	T	0.011	T	GGGCTTGTGTGTTTCAGAGAG CCCCAACAAAAATTCAACCA
rs184491760	9:95,626,888	T	0.016	T	CCCAGAAGAGCTGGACTGAC GAAAAGGGCAGAAGGCAAAT
rs182177904	9:95,800,040	A	0.018	A	AATTGGAAAATGGGCAAGGT CCCAACAGCAGTGTATGAGG

Abbreviation: SNV, single nucleotide variant.

[a]The rare allele and its frequency were determined from the Genome Aggregation Database (gnomAD–Genomes) for Europeans, to most closely reflect the genetic backgrounds of the parents. The details are drawn from dbSNP (https://www.ncbi.nlm.nih.gov/snp/).

(a)

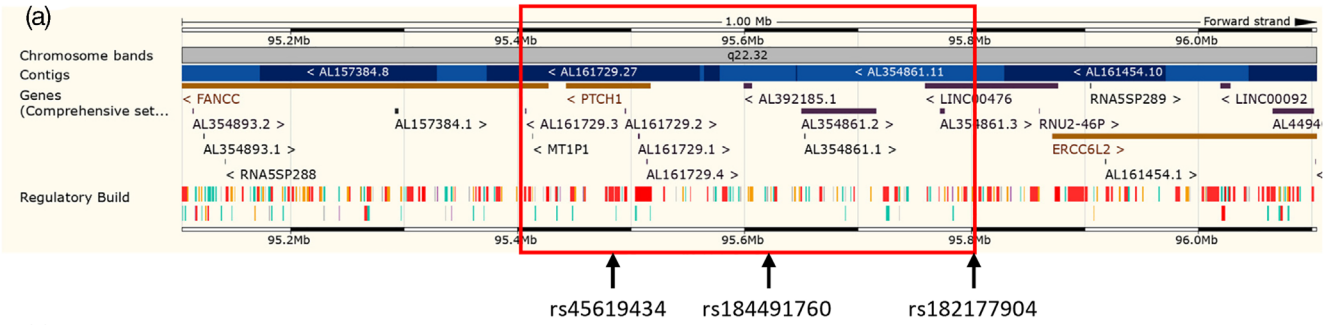

(b)

Gene name	Gene start (bp)	Gene end (bp)	Gene stable ID	Gene description	Transcript type
AL161729.3	95406990	95407662	ENSG00000271384	novel transcript	lncRNA
MT1P1	95413267	95413449	ENSG00000213761	metallothionein 1 pseudogene 1 [Source:HGNC Symbol;Acc:HGNC:23681]	processed_pseudogene
PTCH1	95442980	95517057	ENSG00000185920	patched 1 [Source:HGNC Symbol;Acc:HGNC:9585]	protein_coding
PTCH1	95442980	95517057	ENSG00000185920	patched 1 [Source:HGNC Symbol;Acc:HGNC:9585]	lncRNA
AL161729.2	95494924	95495379	ENSG00000271314	novel transcript, antisense to PTCH1	lncRNA
AL161729.1	95506235	95507636	ENSG00000271155	novel transcript, antisense to PTCH1	lncRNA
AL161729.4	95514045	95514520	ENSG00000271659	novel transcript, antisense to PTCH1	lncRNA
AL392185.1	95599438	95606326	ENSG00000229345	novel transcript	lncRNA
AL354861.2	95650154	95715718	ENSG00000228142	novel transcript	lncRNA
AL354861.1	95652912	95653266	ENSG00000227358	proteasome subunit, alpha type, 7 (PSMA7) pseudogene	processed_pseudogene
LINC00476	95759231	95876049	ENSG00000175611	long intergenic non-protein coding RNA 476 [Source:HGNC Symbol;Acc:HGNC:27858]	lncRNA
AL354861.3	95772323	95776282	ENSG00000268926	novel transcript	lncRNA

FIGURE 2 Chromosome 9 deletion region. (a) Ensembl genome browser image for Chr9:95,100,000-95,700,000. Deleted region is shown in red box. Arrows indicate single nucleotide variants used to identify parent of origin of the deletion. The gene model in Ensembl for *FANCC* extends across all transcripts showing links to the gene, but only two transcripts attributed to this gene, ENST00000433644.2 (*FANCC-203*) and ENST00000636777.1 (*FANCC-212*) lie within the deleted region; the main promoter for *FANCC* lies outside the deletion. See also Figure 4(a) and Supplementary Figure S3. (b) Genes within the deleted region, downloaded using Ensembl BioMart. *PTCH1* is the only protein coding gene annotated in the region. lncRNA, long non-coding RNA [Color figure can be viewed at wileyonlinelibrary.com]

rs235768 (*BMP2*, MIM112261). Of interest, he was heterozygous for rs121908120 (p.Phe228Ile), a predicted pathogenic variant in *WNT10A* (MIM606268) which has been associated with recessive syndromes affecting the teeth and skin (odontoonychodermal dysplasia MIM257980, tooth agenesis, selective, 4 MIM150400, Schopt-Schulz-Passarge syndrome MIM224750). Heterozygotes for Schopt-Schulz-Passarge syndrome have been reported to show dental anomalies (Bohring et al., 2009).

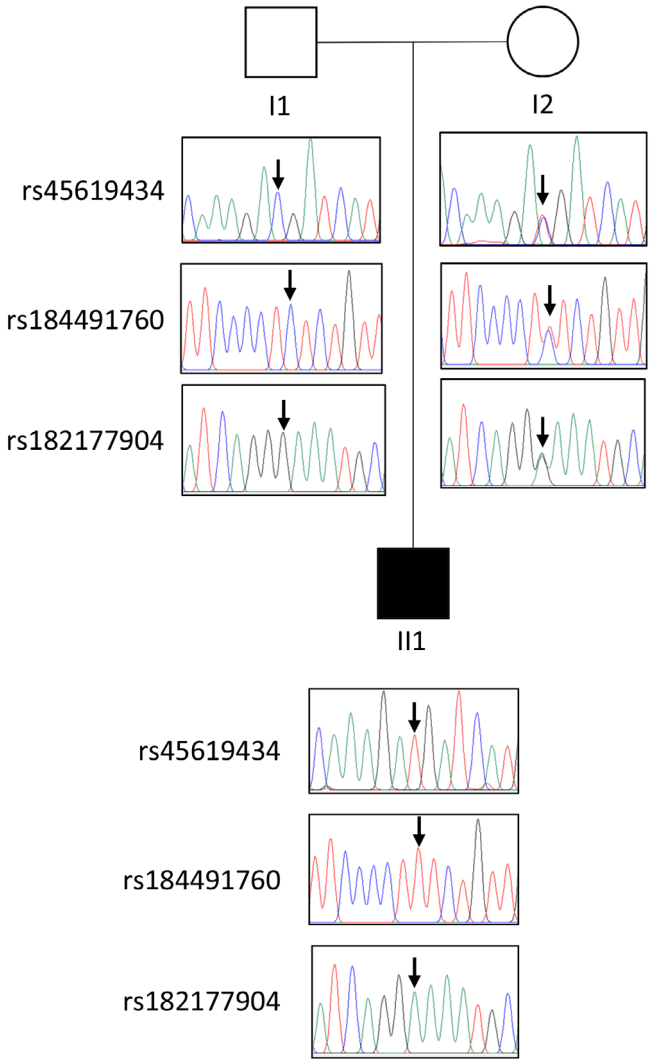

FIGURE 3 Sequence traces for three SNVs used to identify parent of origin. In the pedigree, squares represent males and circles females. The filled-in square shows the proband (individual II1). The mother (I2) is heterozygous at each of the SNVs; the father (I1) is homozygous. The proband has inherited one of the mother's alleles and no allele from the father. SNV, single nucleotide variant [Color figure can be viewed at wileyonlinelibrary.com]

4.3 | Regulatory sequences within the deletion

Another explanation for the severity of his condition would be disrupted interaction between regulatory sequences and their targets where one or other is within the deleted region. The compendium of long-range chromatin interactions published recently (Jung et al., 2019) indicated interactions of sequences within the deletion with *ZNF169*, *FANCC*, *AL354861.3* (formerly known as *DKFZP434H0512*), *ERCC6L2*, *ZNF367*, *HSD17B3*, *HABP4*, *CDC14B*, *PRXL2C* (also known as *AAED1*), and *ZNF510* (from Supplementary Tables 3, 12, and 19 of Jung et al., 2019). Public data for the sequences from within the deletion were also examined to assess possible roles as enhancers. The Enhancer Atlas (Gao et al., 2016) found putative enhancers for *FANCC* and *ERCC6L2* within the deletion and FANTOM5 data (Andersson et al., 2014) also indicated 14 possible enhancers within the deleted region (Figure 4(a)). Consistent with this, GeneHancer analysis from GeneCards showed that sequences within the deletion targeted *FANCC*, *ERCC6L2*, *LINC00476* (partly deleted, overlaps *AL354861.3*), and *EIF4BP3* (Figure 4(b)). These results are summarized in Table 2 and presented in more detail in Supplementary Table S4, with *ERCC6L2* and *FANCC* strongly supported as targets of enhancer activity within the deleted region.

5 | DISCUSSION

We have presented a patient with a microdeletion of chromosome 9 initially detected by MLPA as a deletion of *PTCH1* and then confirmed by CGH and whole genome sequencing to cover approximately 400,000 bases. The deletion encompasses the *PTCH1* gene and several long non-coding RNA genes and pseudogenes, but unlike most other cases of microdeletion 9q22.3 the deletion in our patient does not include the *FANCC* gene. The patient shows an extensive presentation of BCNS in addition to other features commonly seen in longer 9q22.3 deletions but rare in BCNS, such as hydrocephalus and macrosomia (Evans et al., 2017; Muller et al., 2012).

In general, microdeletions result in some form of intellectual disability. This is thought to relate to the high probability of deleting loci involved in neurological development (Schmickel, 1986; Weise et al., 2012). The deletion in our patient is among the shortest reported for this region and he has no intellectual impairment; his academic results are excellent. Although as a young child he had no speech, this was associated with his motor delay and was corrected with specialized speech therapy.

In spite of the short deletion and the presence of only one coding gene (*PTCH1*) within the deletion, our patient has a relatively severe presentation. For example, one 9q22.3 deletion patient (Boonen et al., 2005) had a deletion of 15 megabases (Mb) encompassing 87 genes, but had only 3 BCCs at the age of 21, while our patient with a deletion of less than 1 Mb containing only one coding gene had 58 BCCs and 29 trichoepitheliomas removed by age 16. There are several possible genetic explanations for phenotypic variability in microdeletion syndromes (Srour & Shevell, 2015) which can be applied here. First, the deletion may have unmasked a recessive mutation on the remaining (maternal) allele of *PTCH1* or in the other non-coding transcribed sequences within the deletion. In our analysis, we did not find any potentially pathogenic variant in the remaining *PTCH1* gene, so this explanation seems unlikely. It is more difficult to assess the likely consequences of variants in non-coding sequences, for example, the two variants in the promoter region of *FANCC-203*, but none were obviously pathogenic. Second, alleles at other genes that interact with PTCH1 may influence the phenotype. We looked at variants in the hedgehog pathway genes identified previously (Onodera et al., 2017) and found a number of heterozygous missense mutations that might contribute to the pathology in this patient. In particular, the variant in *WNT10A* has been associated with a tooth agenesis

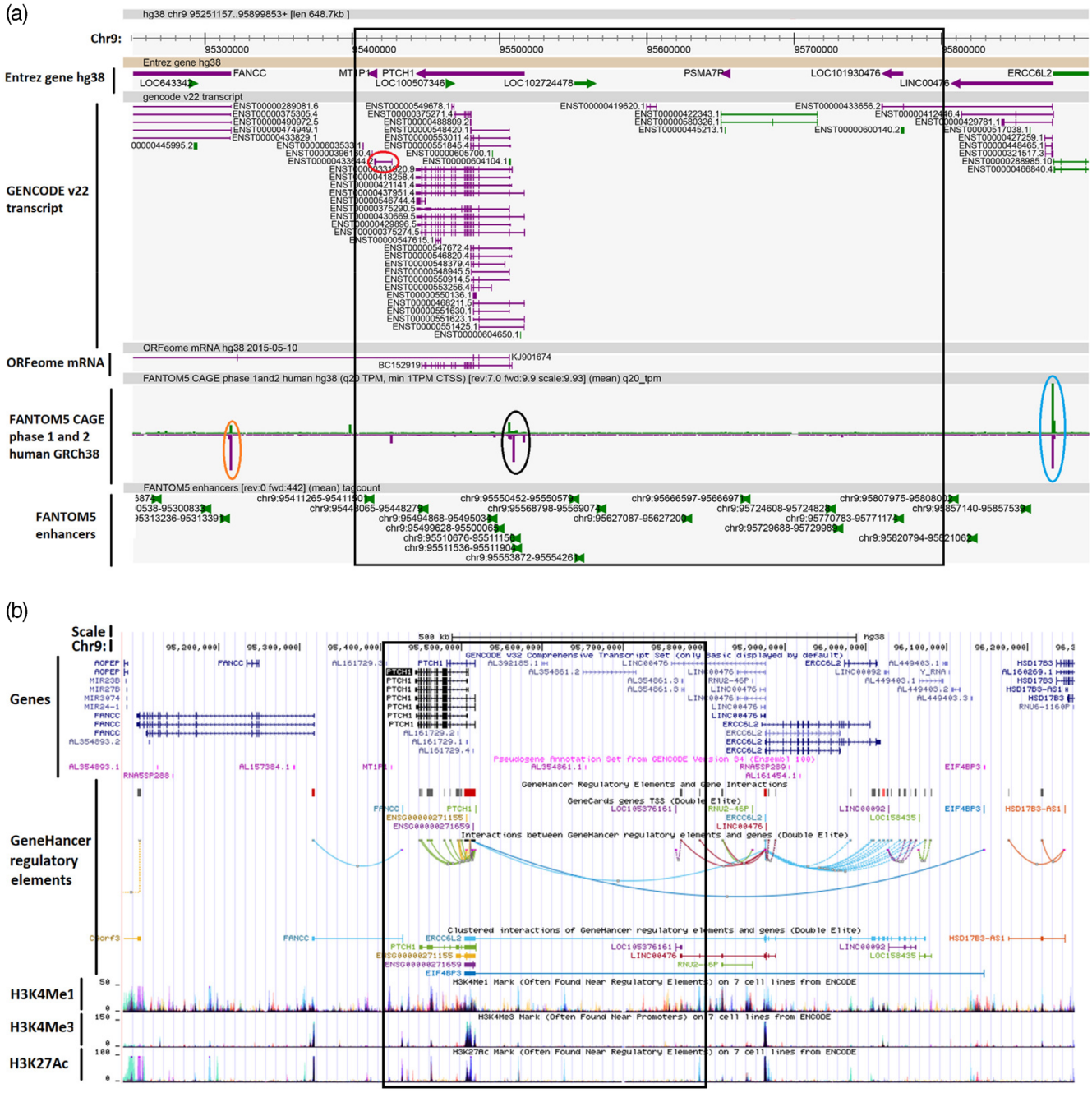

FIGURE 4 Potential regulatory sequences affected by 9q22.3 deletion. (a) FANTOM5 gene expression data. Black box shows the deleted region. Red oval shows *FANCC-203*. Other ovals show promoter regions: black—*PTCH1*; blue—bidirectional promoter for *ERCC6L2* and *LINC00476* (see also Supplementary Figures S6 and S7); orange—*FANCC*. Potential enhancers are shown by the green symbols on the FANTOM5 enhancers track. (b) UCSC Genome Browser view. GeneHancer regulatory elements and histone modifications are shown. H3K4Me1 and H3K27Ac are often found near regulatory elements. H3K4Me3 is often found near promoters [Color figure can be viewed at wileyonlinelibrary.com]

syndrome, accompanied by skin abnormalities. Although generally recessive, this syndrome can manifest in heterozygous individuals (Bohring et al., 2009). It is possible that heterozyosity for the mutation in this gene could exacerbate the *PTCH1* phenotype and this may explain some of our patient's features.

Third, the phenotype may be influenced by epigenetic factors, which is more likely when a phenotype differs depending on the parent of origin as this suggests imprinting. We determined that the paternal chromosome was deleted in this patient. This is consistent with previous reports of 9q22.3 deletions that found all seven patients with overgrowth and macrocephaly had lost the paternal allele (Redon et al., 2006; Shimojima et al., 2009). The possibility of imprinting was suggested. The deletion presented here does not encompass any known imprinted regions but this explanation cannot

TABLE 2 Regulatory relationships between the deleted region and flanking sequences

Target gene	Gene description	Target position	Found by[a]
External targets of sequences within the deletion			
ZNF169	Zinc finger protein 169	9:94,259,298-94,301,829	Compendium of chromatin interactions
FANCC	Fanconi anemia complementation group C	9:95,099,054-95,317,709	EnhancerAtlas, Compendium of chromatin interactions
LINC00476	Long non-coding RNA 00476	9:95,759,231-95,876,049	GeneHancer
ERCC6L2	ERCC excision repair 6 like 2	9:95,871,264-96,121,154	EnhancerAtlas, GeneHancer, Compendium of chromatin interactions
EIF4BP3	Eukaryotic translation initiation factor 4B pseudogene 3	9:96,146,007-96,147,856	GeneHancer
HSD17B3	Hydroxysteroid 17-beta dehydrogenase 3	9:96,235,306-96,302,176	Compendium of chromatin interactions
ZNF367	Zinc finger protein 367	9:96,385,941-96,418,370	Compendium of chromatin interactions
HABP4	Hyaluronan binding protein 4	9:96,450,169-96,491,336	Compendium of chromatin interactions
CDC14B	Cell division cycle 14B	9:96,490,241-96,619,843	Compendium of chromatin interactions
PRXL2C	Peroxiredoxin like 2C (*AAED1*)	9:96,639,577-96,655,317	Compendium of chromatin interactions
ZNF510	Zinc finger protein 510	9:96,755,865-96,778,129	Compendium of chromatin interactions
Target within the deletion of flanking sequences			
FANCC-203	Fanconi anemia complementation group C processed transcript (upstream)	9:95,414,834-95,426,796	GeneHancer

[a]"Found by" indicates the origin of the information: EnhancerAtlas (Gao et al., 2016); GeneHancer (Fishilevich et al., 2017) as implemented in GeneCards (https://www.genecards.org/); Compendium of chromatin interactions (Jung et al., 2019).

be eliminated. However, in general, maternally expressed imprinted genes suppress growth while paternally expressed genes enhance growth (Ishida & Moore, 2013). Therefore, it would be expected that loss of the paternal allele of an imprinted gene would expose the maternal allele and decrease growth, which is in contrast to the reported cases. Yamada and colleagues report a mother and daughter who both have a 4 Mb deletion of 9q22.3 (Yamada et al., 2020). The daughter, who inherited the deletion from her mother and therefore carries the paternal sequence in the deleted region, showed postnatal overgrowth. The parental origin of the deletion in the mother is not revealed.

Finally, the deletion may cause imbalance between a regulator and its target. A recent article (Cappuccio et al., 2019) presented a patient with a microdeletion of chromosome 14 (14q21.1) encompassing a positive regulator of *LRFN5*, a gene outside the deletion that was reduced in expression in the proband. A similar relationship between a sequence within the deletion and its target in the diploid region may explain our patient's presentation. Although there is only one coding sequence within the deletion, there are several other expressed sequences, described as long non-coding RNAs (lncRNAs) or pseudogenes (Figure 2(b)). LncRNAs have been shown to regulate expression (both by silencing and activation) of adjacent or overlapping genes (Gil & Ulitsky, 2020; Liu et al., 2018; Wang et al., 2011; S. Wang et al., 2016). Our analysis of enhancers and chromatin interactions indicated that the most likely targets of sequences within the deletion are *FANCC* and *ERCC6L2* and haploinsufficiency for the deleted sequences may result in over- or underexpression of these and other potential target genes. *PTCH1*, *ERCC6L2*, *LINC00476*, and *FANCC* are highly expressed in the osteosarcoma cell line SAOS-2 undergoing mineralization (Supplementary Figures S4–S7), and dysregulation of these genes could contribute to the skeletal phenotype in this patient. Loci containing *let-7* family microRNAs are frequently within 9q22.3 deletions and have been implicated in aspects of the phenotype (Yamada et al., 2020) but these sequences, at around 9:94,220,000, are outside the deletion in the present patient. A recent article (Liu et al., 2020) showed that a sequence within the deletion (designated *RP11-43505.2* in the article, which maps close to *MT1P1* and likely overlaps with *FANCC-203*) is targeted by WNT signaling. Several *WNT* genes are targets of hedgehog signaling (Onodera et al., 2017), and their expression would likely be increased when one copy of *PTCH1* is deleted. However, in this patient one copy of the target gene is also deleted, which may ameliorate or exacerbate the impact of the *PTCH1* deletion.

Although microdeletion 9q22.3 cases usually have a deletion of the *FANCC* gene (Cayrol et al., 2019; Muller et al., 2012), the gene is intact in our patient and he has few manifestations of Fanconi anemia; in some characteristics his phenotype is opposite from those with biallelic *FANCC* mutations. For example, his height, weight, and head circumference have always been greater than the 90th centile for age (Figure 1), while Fanconi anemia patients are characterized by small stature, poor growth, and microcephaly (Schneider et al., 2015). In addition, bone marrow dysfunction means that they have low red blood cell counts, while our patient has recently been diagnosed with polycythaemia. One possibility is that a transcript from within the deletion region usually suppresses the activity of *FANCC*. His extreme phenotype may result in part from an imbalance between *FANCC* and

the putative regulatory transcript, leading to excess activity of *FANCC*, contrasting with Fanconi anemia C patients who have low levels of *FANCC* gene expression from both alleles (as it is a recessive condition). Since most 9q22.3 deletion patients are hemizygous for both loci the balance between the two transcripts would be maintained with no manifestation of overexpression of *FANCC*. Notably, *FANCC* expression is associated with the *FANCC-203* lncRNA promoter by a GeneHancer interaction (Figure 4, Supplementary Figure S3), and this relationship may be disrupted by the deletion of *FANCC-203*. The recent article concerning a microdeletion on chromosome 14 illustrated how deletion of a regulatory sequence can influence a neighboring non-deleted gene (Cappuccio et al., 2019). Another small 9q22.3 deletion was previously reported (Muller et al., 2012). This encompassed *PTCH1* as well as the 5′ end of the *FANCC* gene including the promoter. The patient had similar phenotype but does not appear to be as severely affected as our patient, supporting the idea that deletion of *FANCC-203* (ENST00000433644.2) or another regulatory sequence may cause increased expression of *FANCC*. This would not be found in the second patient who has the promoter region of *FANCC* deleted.

Enhancers for another flanking gene, *ERCC6L2*, were detected in the deleted region (Figure 4). This gene is expressed ubiquitously; FANTOM5 data show expression in a range of cell types (Supplementary Figure S6), including a number of immune cell lineages (granulocyte-macrophage precursors, plasmacytoid dendritic cells, adult and fetal thymus, common myeloid precursor) and some nervous system cells (cerebellum, pituitary). It is also highly expressed in a number of tumor cell types including the osteosarcoma line SAOS-2. The encoded protein, ERCC excision repair 6 like 2, is a helicase which may be involved in nuclear and mitochondrial nucleotide excision repair (Tummala et al., 2018). Patients with biallelic mutations of *ERCC6L2* (MIM615715) have trilineage bone marrow failure, learning disabilities, and microcephaly (Tummala et al., 2014) as well as short stature and other features similar to Fanconi anemia (Jarviaho et al., 2018). Again, this phenotype contrasts with that of our patient, suggesting that negative regulators of this gene may be deleted and the resulting overexpression of *ERCC6L2* may contribute to his condition. Both *ERCC6L2* and *FANCC* are involved in DNA damage repair. Overactivation of one or both due to dysregulation may promote cell proliferation and could explain the macrosomia seen in this patient.

ERCC6L2 is encoded on the forward strand. It has a bidirectional promoter, with the reverse strand transcribed into a long non-coding RNA, *LINC00476*, that is expressed in $CD4^+$ and $CD8^+$ T lymphocyte lineages as well as SAOS-2 cells (Supplementary Figures S7). The deletion affects the 3′ end of one transcript attributed to this gene (*LINC00476-205*; ENST00000433656.2). A variant in this gene was associated with nicotine dependence by genome wide association study (Yin et al., 2017). The association of both *ERCC6L2* and *LINC00476* with neurological and behavioral deficits suggests that they are not important in this patient who has normal intellect and behavior. However, the 5′ end of *LINC00476* would be brought closer to the main *FANCC* promoter (also on the reverse strand) on the deleted chromosome, which may contribute to illegitimate regulation of *FANCC*.

A recent case report presents a patient who was found to be heterozygous for a frame shift mutation (single base insertion) at the beginning of exon 11 of *PTCH1* (p.Val502Gly_fs*13) (Beltrami et al., 2020). Although the mutation affected only *PTCH1*, the patient had some manifestations of 9q22.3 deletion syndrome. The premature termination of translation would disrupt the sterol-sensing domain (amino acids 426–616) within the transmembrane sequence of patched 1. The authors showed that there was also an alteration in mRNA splicing. Thus either through premature termination, removal of the domain by alternative splicing or nonsense mediated decay, it is likely that this patient is haploinsufficient for the sterol-sensing domain as well as transmembrane domains 6–12, containing the large intracellular loop, the second large extracellular loop and the C-terminal cytoplasmic tail of the patched 1 protein. The sterol-sensing domain may be involved in interaction with the hedgehog ligand which is activated by addition of cholesterol and palmitoyl moieties, but has also been shown to bind sterols independently (Qi et al., 2019). This may indicate that patched 1 is involved in sterol translocation across the membrane. Reduced levels of *PTCH1* as in our patient and the truncation of the protein before this point as in the patient discussed above (Beltrami et al., 2020) may explain the extensive phenotype, although other BCNS patients with truncating mutations which would remove this domain but with mild/late onset disease have also been reported (Reinders et al., 2018). Other authors (Wicking et al., 1997) have attributed all the congenital features of BCNS to haploinsufficiency, since the majority of mutations, including some that occur 5′ to the mutation in the patient of Beltrami and colleagues (Beltrami et al., 2020) would result in premature termination (see also (Reinders et al., 2018) and http://www.lovd.nl/). Therefore, it seems unlikely that the severity is due simply to the nature of the *PTCH1* deletion.

An alternative explanation for the high number of skin and jaw lesions is that the patient received repeated doses of ionizing radiation prior to diagnosis of BCNS. This exposure, through X-ray and CT, was received when characterizing the skeletal and jaw phenotype and could have caused numerous additional lesions within the field of exposure and therefore contributed to the more severe lesion phenotype. Children with BCNS are at high risk of developing BCCs at the sites of radiation (reviewed by Kleinerman, 2009), but it is notable that our patient has had no BCCs in the jaw region. Since both flanking genes (*FANCC* and *ERCC6L2*) are involved in DNA repair, a dysregulation of these genes by mechanisms discussed above could interact with the radiation dose to exacerbate radiation sensitivity caused by the loss of *PTCH1*. Such exposure would not account for other features of his phenotype such as macrosomia, hydrocephalus, and skeletal anomalies.

We noted that there is an apparent duplication of sequences in the region with paralogues *ZNF169* and *ZNF510/782*, *NUTM2F* and *NUTM2G*, *YRDCP2* and *YRDCP1*, *RNU6-798P* and *RNU6-669P* either side of the deletion. This may predispose the region to mispairing at meiosis leading to de novo deletion or duplication. The resulting deletions would be larger than that seen in our patient, although repair by gene conversion may have limited the extent.

TABLE 3 Age at presentation and diagnosis of 9q22.3 deletion patients

Presenting age	Age at diagnosis of 9q22.3 deletion	Reference
0	0	Reichert et al., 2015
0	0	Cajaiba et al., 2006)
0	2 weeks	Muller et al., 2012
0	8 weeks	Muller et al., 2012
0	39 weeks	Cayrol et al., 2019
0	3 years 9 months	Shimojima et al., 2009
0	5 years	Redon et al., 2006
0	8 years	Redon et al., 2006
0	9 years	Yamada et al., 2020
0	12 years 6 months	Isidor et al., 2013
0	12 years 9 months	Isidor et al., 2013
0	13 years	Muller et al., 2012
0	14 years	Isidor et al., 2013
0	21 years	Boonen et al., 2005
0	36 years	Kieny et al., 2018
1.5 weeks	1 year	Muller et al., 2012
2 weeks	4 weeks	Muller et al., 2012
6 weeks	10 years 10 months	Present case
12 weeks	39 years	Garavelli et al., 2013
16 weeks	16 weeks	Cayrol et al., 2019
30 weeks	2 years	Muller et al., 2012
39 weeks	2 years	Muller et al., 2012
1 year 1 month	1 year 1 month	Brickler et al., 2014
5 years	11 years	Muller et al., 2012
7 years	7 years	Muller et al., 2012
9 years	9 years	Muller et al., 2012

Finally, in reviewing the literature it became clear that there is a long latency period between presentation of a 9q22.3 microdeletion patient for dysmorphic features or some other complication and detection of the deletion (Table 3). Our patient first presented at age 6 weeks but was not diagnosed with the microdeletion until after the age of 10 years. Others, with severe phenotypes, presented in childhood but the deletion was not detected for more than 30 years. In part, this is due to the development of technologies since the early descriptions of microdeletions in the 1980s (Schmickel, 1986) and it is to be hoped that increasing awareness of the complex phenotypes associated with microdeletions and the new whole genome sequencing approaches will ensure that diagnosis is now made quickly, reducing parental anxiety and potentially leading to more appropriate and more rapid treatment. In addition, early diagnosis of BCNS in these patients would ensure that doses of ionizing radiation were minimized, potentially preventing radiation-induced formation of skin and jaw lesions.

In summary, we present a patient with a short microdeletion within 9q22.3 who has a relatively severe presentation of BCNS (for example, early onset of multiple BCCs and jaw keratocysts) as well as manifestations usually associated with longer 9q22.3 microdeletions (macrosomia, obstructive hydrocephalus). We suggest that the extreme manifestations result from the imbalance of regulators within the deletion and their targets in the diploid region. Further examination of gene expression in this patient should clarify the relationship between the phenotype and the extent of the deletion.

ACKNOWLEDGMENTS

We thank the family for their cooperation and help with this study, and clinicians who have been involved in the care of the patient. The study was partly funded by a private donation to the Mater Foundation. Seth W Cheetham is supported by an Australian National Health and Medical Research Council (NHMRC) Early Career Fellowship (GNT1161832). Adam D Ewing, Seth W Cheetham, and Kim M Summers receive funding from the Mater Foundation, Brisbane, Australia. The Translational Research Institute is supported by the Australian Government.

CONFLICT OF INTEREST

The authors have no conflict of interest to declare.

AUTHOR CONTRIBUTIONS

Adam D Ewing performed the mapping and variant analysis. Seth W Cheetham analyzed the PacBio results for *PTCH1* and *FANCC-203*. James J McGill, Michael Sharkey, and Rick Walker have been involved in diagnosis and clinical care of the patient, Jennifer A West and Malcolm J West were involved in review of the patient, Kim M Summers performed the laboratory and bioinformatic analysis and wrote the manuscript. All authors contributed to and approved the final version of the article.

DATA AVAILABILITY STATEMENT

Variant calls related to the deleted region and hedgehog pathway genes are provided in the Supporting Information. The raw sequence files that support the findings of this study are available on request from the corresponding author. The data are not publicly available due to privacy and ethical restrictions.

ORCID

Kim M. Summers https://orcid.org/0000-0002-7084-4386

REFERENCES

Altaraihi, M., Wadt, K., Ek, J., Gerdes, A. M., & Ostergaard, E. (2019). A healthy individual with a homozygous PTCH2 frameshift variant: Are variants of PTCH2 associated with nevoid basal cell carcinoma syndrome? *Human Genome Variation*, *6*, 10. https://doi.org/10.1038/s41439-019-0041-2

Andersson, R., Gebhard, C., Miguel-Escalada, I., Hoof, I., Bornholdt, J., Boyd, M., Chen, Y., Zhao, X., Schmidl, C., Suzuki, T., Ntini, E., Arner, E., Valen, E., Li, K., Schwarzfischer, L., Glatz, D., Raithel, J., Lilje, B., Rapin, N., … Sandelin, A. (2014). An atlas of active enhancers across human cell types and tissues. *Nature*, *507*, 455–461. https://doi.org/10.1038/nature12787

Beltrami, B., Prada, E., Tolva, G., Scuvera, G., Silipigni, R., Graziani, D., Bulfamante, G., Gervasini, C., Marchisio, P., & Milani, D. (2020). Unexpected phenotype in a frameshift mutation of PTCH1. *Molecular Genetics & Genomic Medicine*, *8*, e987. https://doi.org/10.1002/mgg3.987

Bohring, A., Stamm, T., Spaich, C., Haase, C., Spree, K., Hehr, U., Hoffmann, M., Ledig, S., Sel, S., Wieacker, P., & Röpke, A. (2009). WNT10A mutations are a frequent cause of a broad spectrum of ectodermal dysplasias with sex-biased manifestation pattern in heterozygotes. *American Journal of Human Genetics*, *85*, 97–105. https://doi.org/10.1016/j.ajhg.2009.06.001

Boonen, S. E., Stahl, D., Kreiborg, S., Rosenberg, T., Kalscheuer, V., Larsen, L. A., Tommerup, N., Brøndum-Nielsen, K., & Tümer, Z. (2005). Delineation of an interstitial 9q22 deletion in basal cell nevus syndrome. *American Journal of Medical Genetics. Part A*, *132A*, 324–328. https://doi.org/10.1002/ajmg.a.30422

Brickler, M. M., Basel, D. G., Gheorghe, G., Margolis, D. M., Kelly, M. E., & Ehrhardt, M. J. (2014). Early therapy-related myeloid sarcoma and deletion of 9q22.32 to q31.1. *Pediatric Blood & Cancer*, *61*, 1701–1703. https://doi.org/10.1002/pbc.25040

Cajaiba, M. M., Bale, A. E., Alvarez-Franco, M., McNamara, J., & Reyes-Mugica, M. (2006). Rhabdomyosarcoma, Wilms tumor, and deletion of the patched gene in Gorlin syndrome. *Nature Clinical Practice. Oncology*, *3*, 575–580. https://doi.org/10.1038/ncponc0608

Cappuccio, G., Attanasio, S., Alagia, M., Mutarelli, M., Borzone, R., Karali, M., Genesio, R., Mormile, A., Nitsch, L., Imperati, F., Esposito, A., Banfi, S., del Giudice, E., & Brunetti-Pierri, N. (2019). Microdeletion of pseudogene chr14.232.A affects LRFN5 expression in cells of a patient with autism spectrum disorder. *European Journal of Human Genetics*, *27*, 1475–1480. https://doi.org/10.1038/s41431-019-0430-5

Cayrol, J., Nightingale, M., Challis, J., Campbell, M., Sullivan, M., & Heloury, Y. (2019). Wilms tumor associated with the 9q22.3 microdeletion syndrome: 2 new case reports and a review of the literature. *Journal of Pediatric Hematology/Oncology*, *41*, e517–e520. https://doi.org/10.1097/MPH.0000000000001322

Dimitrieva, S., & Bucher, P. (2013). UCNEbase-a database of ultraconserved non-coding elements and genomic regulatory blocks. *Nucleic Acids Research*, *41*(Database issue, D101–D109. https://doi.org/10.1093/nar/gks1092

Dobbins, T. A., Sullivan, E. A., Roberts, C. L., & Simpson, J. A. (2012). Australian national birthweight percentiles by sex and gestational age, 1998-2007. *The Medical Journal of Australia*, *197*, 291–294.

Dreos, R., Ambrosini, G., Cavin Perier, R., & Bucher, P. (2013). EPD and EPDnew, high-quality promoter resources in the next-generation sequencing era. *Nucleic Acids Research*, *41*(Database issue, D157–D164. https://doi.org/10.1093/nar/gks1233

ENCODE Project Consortium. (2012). An integrated encyclopedia of DNA elements in the human genome. *Nature*, *489*, 57–74. https://doi.org/10.1038/nature11247

Evans, D. G., & Farndon, P. A. (2002). Nevoid basal cell carcinoma syndrome. In M. P. Adam, H. H. Ardinger, & R. A. Pagon (Eds.), *GeneReviews*. Seattle: University of Washington. https://www.ncbi.nlm.nih.gov/books/NBK1151/

Evans, D. G., Oudit, D., Smith, M. J., Rutkowski, D., Allan, E., Newman, W. G., & Lear, J. T. (2017). First evidence of genotype-phenotype correlations in Gorlin syndrome. *Journal of Medical Genetics*, *54*, 530–536. https://doi.org/10.1136/jmedgenet-2017-104669

Fan, Z., Li, J., Du, J., Zhang, H., Shen, Y., Wang, C. Y., & Wang, S. (2008). A missense mutation in PTCH2 underlies dominantly inherited NBCCS in a Chinese family. *Journal of Medical Genetics*, *45*, 303–308. https://doi.org/10.1136/jmg.2007.055343

Fishilevich, S., Nudel, R., Rappaport, N., Hadar, R., Plaschkes, I., Iny Stein, T., Rosen, N., Kohn, A., Twik, M., Safran, M., Lancet, D., & Cohen, D. (2017). GeneHancer: Genome-wide integration of enhancers and target genes in GeneCards. *Database*, *2017*, bax028. https://doi.org/10.1093/database/bax028

Forrest, A. R., Kawaji, H., Rehli, M., Baillie, J. K., de Hoon, M. J., Haberle, V., Lassmann, T., Kulakovskiy, I. V., Lizio, M., Itoh, M., Andersson, R., Mungall, C. J., Meehan, T. F., Schmeier, S., Bertin, N., Jørgensen, M., Dimont, E., Arner, E., Schmidl, C., … Hayashizaki, Y. (2014). A promoter-level mammalian expression atlas. *Nature*, *507*, 462–470. https://doi.org/10.1038/nature13182

Fujii, K., Ohashi, H., Suzuki, M., Hatsuse, H., Shiohama, T., Uchikawa, H., & Miyashita, T. (2013). Frameshift mutation in the PTCH2 gene can cause nevoid basal cell carcinoma syndrome. *Familial Cancer*, *12*, 611–614. https://doi.org/10.1007/s10689-013-9623-1

Gao, T., He, B., Liu, S., Zhu, H., Tan, K., & Qian, J. (2016). EnhancerAtlas: A resource for enhancer annotation and analysis in 105 human cell/tissue types. *Bioinformatics*, *32*, 3543–3551. https://doi.org/10.1093/bioinformatics/btw495

Garavelli, L., Piemontese, M. R., Cavazza, A., Rosato, S., Wischmeijer, A., Gelmini, C., Albertini, E., Albertini, G., Forzano, F., Franchi, F., Carella, M., Zelante, L., & Superti-Furga, A. (2013). Multiple tumor types including leiomyoma and Wilms tumor in a patient with Gorlin syndrome due to 9q22.3 microdeletion encompassing the PTCH1 and FANC-C loci. *American Journal of Medical Genetics. Part A*, *161A*, 2894–2901. https://doi.org/10.1002/ajmg.a.36259

Gibson, R. A., Ford, D., Jansen, S., Savoia, A., Havenga, C., Milner, R. D., de Ravel, T. J., Cohn, R. J., Ball, S. E., & Roberts, I. (1994). Genetic mapping of the FACC gene and linkage analysis in Fanconi anaemia families. *Journal of Medical Genetics*, *31*, 868–871. https://doi.org/10.1136/jmg.31.11.868

Gil, N., & Ulitsky, I. (2020). Regulation of gene expression by cis-acting long non-coding RNAs. *Nature Reviews. Genetics*, *21*, 102–117. https://doi.org/10.1038/s41576-019-0184-5

Gorlin, R. J. (2004). Nevoid basal cell carcinoma (Gorlin) syndrome. *Genetics in Medicine*, *6*, 530–539. https://doi.org/10.1097/01.gim.0000144188.15902.c4

Goudie, D. R., D'Alessandro, M., Merriman, B., Lee, H., Szeverényi, I., Avery, S., O'Connor, B. D., Nelson, S. F., Coats, S. E., Stewart, A., Christie, L., Pichert, G., Friedel, J., Hayes, I., Burrows, N., Whittaker, S., Gerdes, A. M., Broesby-Olsen, S., Ferguson-Smith, M. A., … Lane, E. B. (2011). Multiple self-healing squamous epithelioma is caused by a disease-specific spectrum of mutations in TGFBR1. *Nature Genetics*, *43*, 365–369. https://doi.org/10.1038/ng.780

Ishida, M., & Moore, G. E. (2013). The role of imprinted genes in humans. *Molecular Aspects of Medicine*, *34*, 826–840. https://doi.org/10.1016/j.mam.2012.06.009

Isidor, B., Bourdeaut, F., Lafon, D., Plessis, G., Lacaze, E., Kannengiesser, C., Rossignol, S., Pichon, O., Briand, A., Martin-Coignard, D., Piccione, M., David, A., Delattre, O., Jeanpierre, C., Sévenet, N., & le Caignec, C. (2013). Wilms' tumor in patients with 9q22.3 microdeletion syndrome suggests a role for PTCH1 in nephroblastomas. *European Journal of Human Genetics*, *21*, 784–787. https://doi.org/10.1038/ejhg.2012.252

Jarviaho, T., Halt, K., Hirvikoski, P., Moilanen, J., Mottonen, M., & Niinimaki, R. (2018). Bone marrow failure syndrome caused by homozygous frameshift mutation in the ERCC6L2 gene. *Clinical Genetics*, *93*, 392–395. https://doi.org/10.1111/cge.13125

Jung, I., Schmitt, A., Diao, Y., Lee, A. J., Liu, T., Yang, D., Tan, C., Eom, J., Chan, M., Chee, S., Chiang, Z., Kim, C., Masliah, E., Barr, C. L., Li, B., Kuan, S., Kim, D., & Ren, B. (2019). A compendium of promoter-centered long-range chromatin interactions in the human genome. *Nature Genetics*, *51*, 1442–1449. https://doi.org/10.1038/s41588-019-0494-8

Khan, A., & Zhang, X. (2016). dbSUPER: A database of super-enhancers in mouse and human genome. *Nucleic Acids Research*, *44*(D1), D164–D171. https://doi.org/10.1093/nar/gkv1002

Kieny, A., Kremer, V., Scheidecker, S., & Lipsker, D. (2018). 9q22.3 microdeletion syndrome with multiple basal cell carcinomas treated with Vismodegib: Three key messages in one patient. *Acta Dermato-Venereologica*, *98*, 287–288. https://doi.org/10.2340/00015555-2822

Kieran, M. W., Chisholm, J., Casanova, M., Brandes, A. A., Aerts, I., Bouffet, E., Bailey, S., Leary, S., MacDonald, T., Mechinaud, F., Cohen, K. J., Riccardi, R., Mason, W., Hargrave, D., Kalambakas, S., Deshpande, P., Tai, F., Hurh, E., & Geoerger, B. (2017). Phase I study of oral sonidegib (LDE225) in pediatric brain and solid tumors and a phase II study in children and adults with relapsed medulloblastoma. *Neuro-Oncology*, *19*, 1542–1552. https://doi.org/10.1093/neuonc/nox109

Kleinerman, R. A. (2009). Radiation-sensitive genetically susceptible pediatric sub-populations. *Pediatric Radiology*, *39*(Suppl 1), S27–S31. https://doi.org/10.1007/s00247-008-1015-6

Landrum, M. J., & Kattman, B. L. (2018). ClinVar at five years: Delivering on the promise. *Human Mutation*, *39*, 1623–1630. https://doi.org/10.1002/humu.23641

Landrum, M. J., Lee, J. M., Benson, M., Brown, G. R., Chao, C., Chitipiralla, S., Gu, B., Hart, J., Hoffman, D., Jang, W., Karapetyan, K., Katz, K., Liu, C., Maddipatla, Z., Malheiro, A., McDaniel, K., Ovetsky, M., Riley, G., Zhou, G., … Maglott, D. R. (2018). ClinVar: Improving access to variant interpretations and supporting evidence. *Nucleic Acids Research*, *46*(D1), D1062–D1067. https://doi.org/10.1093/nar/gkx1153

Li, H. (2013). Aligning sequence reads, clone sequences and assembly contigs with BWA-MEM. *arXiv*, *1303*, 3997v2 [q-bio.GN].

Liu, C., Li, C., Deng, Z., Du, E., & Xu, C. (2018). Long non-coding RNA BC168687 is involved in TRPV1-mediated diabetic neuropathic pain in rats. *Neuroscience*, *374*, 214–222. https://doi.org/10.1016/j.neuroscience.2018.01.049

Liu, S., Harmston, N., Glaser, T. L., Wong, Y., Zhong, Z., Madan, B., Virshup, D. M., & Petretto, E. (2020). Wnt-regulated lncRNA discovery enhanced by in vivo identification and CRISPRi functional validation. *Genome Medicine*, *12*, 89. https://doi.org/10.1186/s13073-020-00788-5

Loeys, B. L., Chen, J., Neptune, E. R., Judge, D. P., Podowski, M., Holm, T., Meyers, J., Leitch, C. C., Katsanis, N., Sharifi, N., Xu, F. L., Myers, L. A., Spevak, P. J., Cameron, D. E., de Backer, J., Hellemans, J., Chen, Y., Davis, E. C., Webb, C. L., … Dietz, H. C. (2005). A syndrome of altered cardiovascular, craniofacial, neurocognitive and skeletal development caused by mutations in TGFBR1 or TGFBR2. *Nature Genetics*, *37*, 275–281. https://doi.org/10.1038/ng1511

Malbari, F., & Lindsay, H. (2020). Genetics of common pediatric brain tumors. *Pediatric Neurology*, *104*, 3–12. https://doi.org/10.1016/j.pediatrneurol.2019.08.004

McKenna, A., Hanna, M., Banks, E., Sivachenko, A., Cibulskis, K., Kernytsky, A., Garimella, K., Altshuler, D., Gabriel, S., Daly, M., & DePristo, M. A. (2010). The genome analysis toolkit: A MapReduce framework for analyzing next-generation DNA sequencing data. *Genome Research*, *20*, 1297–1303. https://doi.org/10.1101/gr.107524.110

McLaren, W., Gil, L., Hunt, S. E., Riat, H. S., Ritchie, G. R., Thormann, A., Flicek, P., & Cunningham, F. (2016). The Ensembl variant effect predictor. *Genome Biology*, *17*, 122. https://doi.org/10.1186/s13059-016-0974-4

Muller, E. A., Aradhya, S., Atkin, J. F., Carmany, E. P., Elliott, A. M., Chudley, A. E., Clark, R. D., Everman, D. B., Garner, S., Hall, B. D., Herman, G. E., Kivuva, E., Ramanathan, S., Stevenson, D. A., Stockton, D. W., & Hudgins, L. (2012). Microdeletion 9q22.3 syndrome includes metopic craniosynostosis, hydrocephalus, macrosomia, and developmental delay. *American Journal of Medical Genetics. Part A*, *158A*, 391–399. https://doi.org/10.1002/ajmg.a.34216

Onodera, S., Saito, A., Hasegawa, D., Morita, N., Watanabe, K., Nomura, T., Shibahara, T., Ohba, S., Yamaguchi, A., & Azuma, T. (2017). Multilayered mutation in hedgehog-related genes in Gorlin syndrome may affect the phenotype. *PLoS One*, *12*, e0184702. https://doi.org/10.1371/journal.pone.0184702

Pastorino, L., Ghiorzo, P., Nasti, S., Battistuzzi, L., Cusano, R., Marzocchi, C., Garrè, M. L., Clementi, M., & Scarrà, G. B. (2009). Identification of a SUFU germline mutation in a family with Gorlin syndrome. *American Journal of Medical Genetics. Part A*, *149A*, 1539–1543. https://doi.org/10.1002/ajmg.a.32944

Qi, C., Di Minin, G., Vercellino, I., Wutz, A., & Korkhov, V. M. (2019). Structural basis of sterol recognition by human hedgehog receptor PTCH1. *Science Advances*, *5*, eaaw6490. https://doi.org/10.1126/sciadv.aaw6490

Rausch, T., Zichner, T., Schlattl, A., Stutz, A. M., Benes, V., & Korbel, J. O. (2012). DELLY: Structural variant discovery by integrated paired-end and split-read analysis. *Bioinformatics*, *28*, i333–i339. https://doi.org/10.1093/bioinformatics/bts378

Redon, R., Baujat, G., Sanlaville, D., le Merrer, M., Vekemans, M., Munnich, A., Carter, N. P., Cormier-Daire, V., & Colleaux, L. (2006). Interstitial 9q22.3 microdeletion: Clinical and molecular characterisation of a newly recognised overgrowth syndrome. *European Journal of Human Genetics*, *14*, 759–767. https://doi.org/10.1038/sj.ejhg.5201613

Reichert, S. C., Zelley, K., Nichols, K. E., Eberhard, M., Zackai, E. H., & Martinez-Poyer, J. (2015). Diagnosis of 9q22.3 microdeletion syndrome in utero following identification of craniosynostosis, overgrowth, and skeletal anomalies. *American Journal of Medical Genetics. Part A*, *167A*, 862–865. https://doi.org/10.1002/ajmg.a.37013

Reinders, M. G., van Hout, A. F., Cosgun, B., Paulussen, A. D., Leter, E. M., Steijlen, P. M., Mosterd, K., van Geel, M., & Gille, J. J. (2018). New mutations and an updated database for the patched-1 (PTCH1) gene. *Molecular Genetics & Genomic Medicine*, *6*, 409–415. https://doi.org/10.1002/mgg3.380

Robinson, G. W., Kaste, S. C., Chemaitilly, W., Bowers, D. C., Laughton, S., Smith, A., Gottardo, N. G., Partap, S., Bendel, A., Wright, K. D., Orr, B. A., Warner, W. C., Onar-Thomas, A., & Gajjar, A. (2017). Irreversible growth plate fusions in children with medulloblastoma treated with a targeted hedgehog pathway inhibitor. *Oncotarget*, *8*, 69295–69302. https://doi.org/10.18632/oncotarget.20619

Schmickel, R. D. (1986). Contiguous gene syndromes: A component of recognizable syndromes. *The Journal of Pediatrics*, *109*, 231–241.

Schneider, M., Chandler, K., Tischkowitz, M., & Meyer, S. (2015). Fanconi anaemia: Genetics, molecular biology, and cancer - implications for clinical management in children and adults. *Clinical Genetics*, *88*, 13–24. https://doi.org/10.1111/cge.12517

Shimojima, K., Adachi, M., Tanaka, M., Tanaka, Y., Kurosawa, K., & Yamamoto, T. (2009). Clinical features of microdeletion 9q22.3 (pat). *Clinical Genetics*, *75*, 384–393. https://doi.org/10.1111/j.1399-0004.2008.01141.x

Soufir, N., Gerard, B., Portela, M., Brice, A., Liboutet, M., Saiag, P., Descamps, V., Kerob, D., Wolkenstein, P., Gorin, I., Lebbe, C., Dupin, N., Crickx, B., Basset-Seguin, N., & Grandchamp, B. (2006). PTCH mutations and deletions in patients with typical nevoid basal cell carcinoma syndrome and in patients with a suspected genetic predisposition to basal cell carcinoma: A French study. *British Journal of Cancer*, *95*, 548–553. https://doi.org/10.1038/sj.bjc.6603303

Srour, M., & Shevell, M. (2015). Global developmental delay and intellectual disability. In R. N. Rosenberg & J. M. Pascual (Eds.), *Rosenberg's molecular and genetic basis of neurological and psychiatric disease* (5th

ed.). London: Academic Press. https://doi.org/10.1016/B978-0-12-410529-4.09993-9.

Thalakoti, S., & Geller, T. (2015). Basal cell nevus syndrome or Gorlin syndrome. *Handbook of Clinical Neurology*, *132*, 119–128. https://doi.org/10.1016/B978-0-444-62702-5.00008-1

Tummala, H., Dokal, A. D., Walne, A., Ellison, A., Cardoso, S., Amirthasigamanipillai, S., Kirwan, M., Browne, I., Sidhu, J. K., Rajeeve, V., Rio-Machin, A., Seraihi, A. A., Duncombe, A. S., Jenner, M., Smith, O. P., Enright, H., Norton, A., Aksu, T., Özbek, N. Y., … Vulliamy, T. (2018). Genome instability is a consequence of transcription deficiency in patients with bone marrow failure harboring biallelic ERCC6L2 variants. *Proceedings of the National Academy of Sciences of the United States of America*, *115*, 7777–7782. https://doi.org/10.1073/pnas.1803275115

Tummala, H., Kirwan, M., Walne, A. J., Hossain, U., Jackson, N., Pondarre, C., Plagnol, V., Vulliamy, T., & Dokal, I. (2014). ERCC6L2 mutations link a distinct bone-marrow-failure syndrome to DNA repair and mitochondrial function. *American Journal of Human Genetics*, *94*, 246–256. https://doi.org/10.1016/j.ajhg.2014.01.007

Visel, A., Minovitsky, S., Dubchak, I., & Pennacchio, L. A. (2007). VISTA enhancer browser-a database of tissue-specific human enhancers. *Nucleic Acids Research*, *35*(Database issue, D88–D92. https://doi.org/10.1093/nar/gkl822

Wang, K. C., Yang, Y. W., Liu, B., Sanyal, A., Corces-Zimmerman, R., Chen, Y., Lajoie, B. R., Protacio, A., Flynn, R. A., Gupta, R. A., Wysocka, J., Lei, M., Dekker, J., Helms, J. A., & Chang, H. Y. (2011). A long noncoding RNA maintains active chromatin to coordinate homeotic gene expression. *Nature*, *472*, 120–124. https://doi.org/10.1038/nature09819

Wang, S., Xu, H., Zou, L., Xie, J., Wu, H., Wu, B., Yi, Z., Lv, Q., Zhang, X., Ying, M., Liu, S., Li, G., Gao, Y., Xu, C., Zhang, C., Xue, Y., & Liang, S. (2016). LncRNA uc.48+ is involved in diabetic neuropathic pain mediated by the P2X3 receptor in the dorsal root ganglia. *Purinergic Signal*, *12*, 139–148. https://doi.org/10.1007/s11302-015-9488-x

Weise, A., Mrasek, K., Klein, E., Mulatinho, M., Jr Llerena, J. C., Hardekopf, D., Pekova, S., Bhatt, S., Kosyakova, N., & Liehr, T. (2012). Microdeletion and microduplication syndromes. *The Journal of Histochemistry and Cytochemistry*, *60*, 346–358. https://doi.org/10.1369/0022155412440001

Wicking, C., Shanley, S., Smyth, I., Gillies, S., Negus, K., Graham, S., Suthers, G., Haites, N., Edwards, M., Wainwright, B., & Chenevix-Trench, G. (1997). Most germ-line mutations in the nevoid basal cell carcinoma syndrome lead to a premature termination of the PATCHED protein, and no genotype-phenotype correlations are evident. *American Journal of Human Genetics*, *60*, 21–26.

Wilderman, A., VanOudenhove, J., Kron, J., Noonan, J. P., & Cotney, J. (2018). High-resolution Epigenomic atlas of human embryonic craniofacial development. *Cell Reports*, *23*, 1581–1597. https://doi.org/10.1016/j.celrep.2018.03.129

Yamada, H., Shimura, M., Takahashi, H., Nara, S., Morishima, Y., Go, S., Miyashita, T., Numabe, H., & Kawashima, H. (2020). A familial case of overgrowth syndrome caused by a 9q22.3 microdeletion in a mother and daughter. *European Journal of Medical Genetics*, *63*, 103872. https://doi.org/10.1016/j.ejmg.2020.103872

Yin, X., Bizon, C., Tilson, J., Lin, Y., Gizer, I. R., Ehlers, C. L., & Wilhelmsen, K. C. (2017). Genome-wide meta-analysis identifies a novel susceptibility signal at CACNA2D3 for nicotine dependence. *American Journal of Medical Genetics. Part B, Neuropsychiatric Genetics*, *174*, 557–567. https://doi.org/10.1002/ajmg.b.32540

Zerbino, D. R., Wilder, S. P., Johnson, N., Juettemann, T., & Flicek, P. R. (2015). The ensembl regulatory build. *Genome Biology*, *16*, 56. https://doi.org/10.1186/s13059-015-0621-5

SUPPORTING INFORMATION

Additional supporting information may be found online in the Supporting Information section at the end of this article.

How to cite this article: Ewing, A. D., Cheetham, S. W., McGill, J. J., Sharkey, M., Walker, R., West, J. A., West, M. J., Summers, K. M.. Microdeletion of 9q22.3: A patient with minimal deletion size associated with a severe phenotype. *Am J Med Genet Part A*. 2021;*185*A:2070–2083. https://doi.org/10.1002/ajmg.a.62224